# Rapid whole-genome based typing and surveillance of avipoxviruses using nanopore sequencing.

Guillaume Croville, Guillaume Le Loc'H, Catherine Zanchetta, Maxime Manno, Christelle Camus-Bouclainville, Christophe Klopp, Maxence Delverdier, Marie-Noêlle Lucas, Cecile Donnadieu, Mattias Delpont, et al.

Journal of Virological Methods 261 (2018) 34–39

Contents lists available at ScienceDirect

Journal of Virological Methods

journal homepage: www.elsevier.com/locate/jviromet

# Rapid whole-genome based typing and surveillance of avipoxviruses using nanopore sequencing

Guillaume Croville[a], Guillaume Le Loc'h[a], Catherine Zanchetta[b], Maxime Manno[b], Christelle Camus-Bouclainville[a], Christophe Klopp[c], Maxence Delverdier[a], Marie-Noëlle Lucas[a], Cécile Donnadieu[b], Mattias Delpont[a], Jean-Luc Guérin[a,*]

[a] Université de Toulouse, ENVT, INRA, UMR 1225, 31076 Toulouse, France
[b] GeT-PlaGe, INRA, Genotoul, US1426, 31326, Castanet-Tolosan Cedex, France
[c] Plateforme Bioinformatique Genotoul, UR875, Biométrie et Intelligence Artificielle, INRA, Castanet-Tolosan, France

ARTICLE INFO

*Keywords:*
Fowlpox
Poxvirus
Next-generation sequencing
Oxford nanopore MinION
Whole-genome surveillance

ABSTRACT

Avian pox is an infectious disease caused by avipoxviruses (APV), resulting in cutaneous and/or tracheal lesions. Poxviruses share large genome sizes (from 130 to 360 kb), featuring repetitions, deletions or insertions as a result of a long-term recombination history.

The increasing performances of next-generation sequencing (NGS) opened new opportunities for surveillance of poxviruses, based on timely and affordable workflows. We investigated the application of the 3rd generation Oxford Nanopore Minion technology to achieve real-time whole-genome sequencing directly from lesions, without any enrichment or isolation step.

Fowlpox lesions were sampled on hens, total DNA was extracted and processed for sequencing on a MinION, Oxford Nanopore. We readily generated whole APV genomes from cutaneous or tracheal lesions, without any isolation or PCR-based enrichment: Fowlpox virus reads loads ranged from 0.75% to 2.62% and reads up to 61 kbp were generated and readily assembled into 3 APV complete genomes. This long read size eases the assembly step and lowers the bioinformatics capacity requirements and processing time compared to huge sets of short reads. The complete genome analysis confirmed that these Fowlpox viruses cluster within clade A1 and host full length reticuloendotheliovirus (REV) inserts. The pathobiological relevance of REV insert, although a classical feature of fowlpoxviruses (FPVs), should be further investigated. Surveillance of emerging poxviruses could greatly benefit from real-time whole genome sequencing.

## 1. Introduction

Avian pox is an infectious disease caused by avipoxviruses (APV), resulting in cutaneous and/or tracheal lesions. This condition may have a major economic impact in gallinaceous poultry (Zhao et al., 2014) and is an emerging concern for wildlife, as evidenced for British great tits (Lawson et al., 2012). Fowlpox is caused by different clades of avipoxviruses, the most important being clade A (fowlpox viruses) and clade B (canarypox viruses), both showing much more intra-clade genetic variability than previously assumed (Bányai et al., 2015; Gyuranecz et al., 2013; Le Loc'h et al., 2014). Poxviruses share large genome sizes (from 130 to 360 kb) (Lefkowitz et al., 2006), featuring repetitions, deletions or insertions as a result of a long-term recombination history.

So far, avian pox diagnosis and surveillance are based on histopathological identification of typical cytoplasmic inclusions, isolation on chorioallantoid membrane (CAM) of chicken embryos and PCR targeting one or multiple viral genes (Lecis et al., 2017). Very few APV whole genomes are available so far in public databases (i.e. 7 complete genomes of in NCBI GenBank as of the 30th of August 2017). The increasing performances of next-generation sequencing (NGS) opened new opportunities for surveillance of poxviruses, based on timely and affordable workflows. One major drawback of 1st and 2nd generation NGS technologies is their limited read length, making the assembly of complex and large viral genomes very difficult. We investigated the application of the 3rd generation Oxford Nanopore Minion technology to achieve real-time whole-genome sequencing directly from lesions, without any enrichment or isolation step.

* Corresponding author.
*E-mail address:* jl.guerin@envt.fr (J.-L. Guérin).

https://doi.org/10.1016/j.jviromet.2018.08.003
Received 12 January 2018; Received in revised form 22 July 2018; Accepted 3 August 2018
Available online 04 August 2018
0166-0934/ 

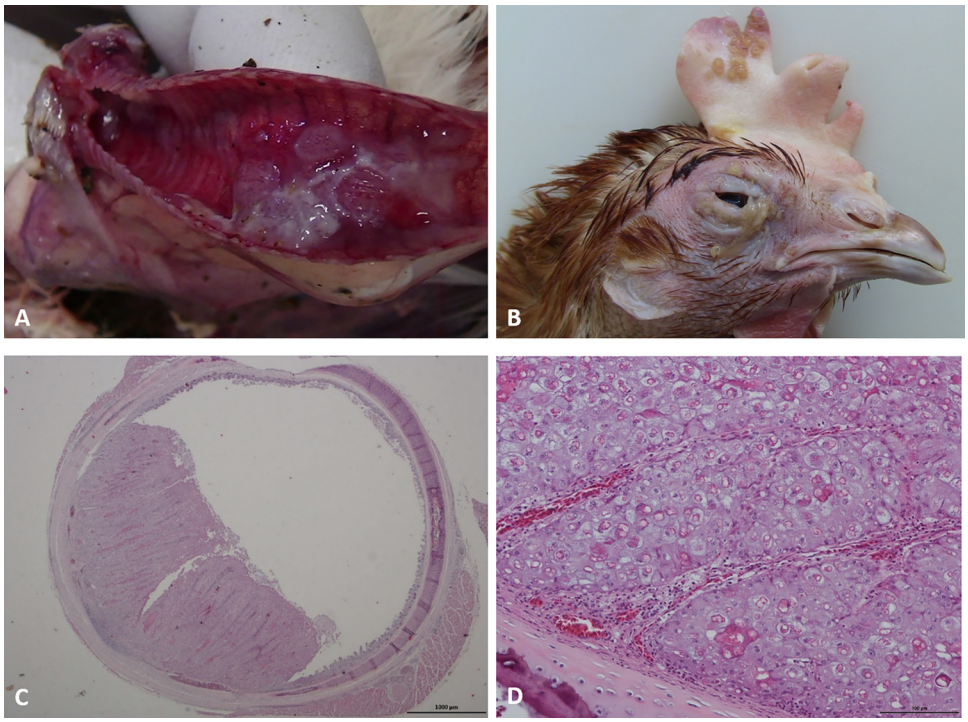


**Fig. 1.** Pathological appearance of fowlpox cases. Gross lesions of respiratory (1A) and cutaneous fowlpox (1B); note hyperplastic nodules coated by a fibrino-necrotic exudate on the trachea (1A), and small and coalescent proliferative lesions on the comb and eyelids (1B). Microscopic lesions of respiratory pox: severe proliferative, hyperplastic and metaplastic, incompletely obstructive lesion of the tracheal mucosa (x20 magnification, 1C) with numerous typical cytoplasmic eosinophilic inclusions (arrows) (x200 magnification, 1D).

## 2. Material and methods

### 2.1. Case history, clinical examination and sampling

In spring 2016, avian pox was diagnosed in a commercial layer farm in Pays de la Loire, France. The affected flock (60,000 birds) showed very good management and biosecurity. Mortality increased suddenly and reached 2% daily. Diseased birds developed severe dyspnea and suffocation before death. This farm was sampled twice, at 3-month interval, under submission numbers 16-055 and 16-069. The main macroscopic lesion was a very severe hyperplastic and necrotizing tracheitis (Fig. 1A). Almost no cutaneous lesion could be observed in any bird.

Two independent broilers breeders farms (cases #16-117 and #16-130, 17,000 and 2500 birds, respectively) were diagnosed in fall 2016 for cutaneous fowlpox in Occitanie, France. Affected birds showed conjunctivitis and nodular hyperplastic lesions on combs and wattles (Fig. 1B), moderate egg drop and mild to moderate mortality.

All these flocks were submitted to a complete clinical examination, including comprehensive necropsy of at least 10 birds per flock. Selected birds were specifically necropsied for tissue sampling: sections of nodular cutaneous and/or tracheal tissues were sampled and stored at −80 °C for virus isolation and/or molecular assays.

### 2.2. Virus isolation on chicken embryos

For virus isolation, a lesion was grounded with sterile quartz using pestle and mortar and then suspended in phosphate-buffered saline containing 200 IU/ml penicillin and 200 mg/ml streptomycin. After centrifugation (100*g* for 10 min), 100 µl of 1:5 diluted supernatant was inoculated on the chorioallantoic membranes (CAMs) of specific-pathogen free 11-day-old chicken embryos. Inoculated eggs were incubated at 37 °C for 7 days and then CAMs presenting pocks were sampled.

### 2.3. DNA extraction

A total of 8 DNA extractions were performed from the tissue culture or directly from the 7 collected lesions: tracheal tissue (n = 2), lung tissue (n = 1), central nodular cutaneous tissue (n = 2), peripheral nodular cutaneous tissue (n = 2). The extraction protocol was derived from Sambrook and Russell, 2001. Briefly, tissue pieces were incubated in SNET lysis buffer (made of Tris-Cl, EDTA, NaCl, SDS and TE) supplemented with proteinase K at a 0,4 mg/ml final concentration. Then, the preparation was incubated overnight at 55 °C with agitation in a shaking incubator. After RNase A treatment following manufacturer's instructions (ThermoFisher scientific), the DNA extraction was performed using phenol:chloroform:isoamyl alcohol (25:24:1, v/v), then the extracted DNA was precipitated by adding isopropanol before pelleting by centrifugation. DNA recovery was achieved through rinsing with 70% ethanol and dissolving in TE. DNA quantitation for each sample was done by OD measurement and the purity of the solution was estimated considering the 260/280 ratio which is supposed to average 1.8 for a pure DNA solution. After that, DNA samples were directly submitted to MinION library preparation without any enrichment step.

### 2.4. Avipoxvirus specific PCR

Avipoxvirus were systematically tested using primers targeting *p4b* locus (Huw Lee and Hwa Lee, 1997). The PCR mixtures were performed using KAPA2G Robust PCR kit (Kapa Biosystems, Roche Holding AG, Basel, Switzerland) and contained 15.9 µl of distilled water, 5 µl of 5x KAPA2G buffer A, 0.5 µl of 10 mmol/liter KAPA dNTP mix, 1.25 µl of 10 µmol/liter P1 primer (5′-CAGCAGGTGCTAAACAACAA-3′) and 1.25 µl of 10 µmol/liter P2 primer (5′-CGGTAGCTTAACGCCGAATA-3′), 0.1 µl of KAPA2G Robust DNA polymerase and 1 µl of DNA. The amplification program consisted of a first 3-minute step at 95 °C followed by 35 cycles with the following conditions: 95 °C for 20 s, 58 °C for 20 s and 72 °C for 20 s. The program ended with 1 step at 72 °C for 5 min. The size of amplified DNA fragment was expected to be 578-pb long.

### 2.5. MinION library preparation

Samples were prepared for sequencing following the 1D Native barcoding genomic DNA protocol (EXP-NBD103 and SQK-LSK108, ONT). 1.7 µg DNA was sheared in a Covaris g-TUBE centrifuged at

7200 rpm for 2 min, inverting the tube between centrifugation steps. Then, a 0.4X AMPure beads purification has been performed. DNA repair, end repair and A-tailing (M6630 and E7546, NEB) were performed on DNA (average size of 8 kb), each step followed by a 0.5X AMPure beads purification. Native barcodes have been ligated using the Blunt/TA ligase master mix (M0367, NEB). Equimolar amounts of each barcoded sample have been pooled to obtain a 700 ng final quantity (~0.13pmols of DNA). Adapters have been ligated using the NEBNext Quick ligation Module (E7546, NEB). A 1X AMPure beads purification followed both of the ligation steps.

### 2.6. MinION sequencing

MinION sequencing was performed as per manufacturer's guidelines using R9.4 flowcells (FLO-MIN106, ONT) and ran for up to 48 h. Three runs were performed for: (i) DNA extracted from CAM-amplified virus, (ii) DNA extracted from respiratory lesion 16069-1, peripheral nodular cutaneous tissue 16130-3, peripheral nodular cutaneous tissue 16117-2, (iii) cutaneous lesion 16117-1, respiratory lesion 16055-3, Cutaneous lesion 16130-2, respiratory lesion (lung) 16055-1. The MUX scan reported 1298, 1350 and 1434 active pores for each flowcell respectively. The computer specifications to ensure the MinION sequencing was: processor Intel(R) Core(TM) i7-6700, CPU @ 3.40 GHz, 8 cores. 16GB Memory. SSD 500GB.

### 2.7. Data analysis

The raw sequence data under fast5 format was loaded to Albacore (v1.1.0) for base calling and demultiplexing. After being extracted from the fast5 files by Poretools (Loman and Quinlan, 2014), each fastq file obtained was aligned against the avipox genome NC_002188.1 employed as a reference using BWA-MEM (Li and Durbin, 2009) with default stringency parameters and the alignments were manipulated with the SAMtools software package (Li et al., 2009). The resulting sorted files were then displayed within the IGV browser (Robinson et al., 2011). Basic statistics concerning the aligned sequences were obtained by analysis of the bam files using FastQC (http://www.bioinformatics.babraham.ac.uk/projects/fastqc/). Reads mapping fowlpox virus genome and the mean sequencing depth were counted with the flagstat option and the depth option of the SAMtools, respectively. Consensus sequence was generated by the IGV browser whose method is derived from Cavener, 1987.

Each consensus sequence was annotated with GATU (Tcherepanov et al., 2006), using Fowlpox virus genome NC_002188.1 as a reference, and deposited in GenBank.

Whole genomes sequences were aligned with whole genomes available on GenBank (n = 8) using method FFT-NS-2 implemented in MAFFT version 7 software (Katoh et al., 2002). A phylogenetic analysis was then performed using MEGA 7 by neighbor-joining with the Kimura 2-parameters model and trees were tested through 1000 bootstrap replicates.

*De novo* assemblies were performed using SMARTdenovo (Ruan, 2018) or Minimap2 (Li, 2017) with default stringency parameters. In addition, we used Racon (Vaser et al., 2017) which is a consensus module for raw de novo DNA assembly of long uncorrected reads.

Error rates were estimated using BLASR tool and its –m 1 option generating percentage similarity between the reads and a reference genome.

## 3. Results

### 3.1. Pathological and virological observations

Representative samples from all flocks were submitted to a comprehensive pathological investigation and tissue sampling. Histopathology performed on tracheal and cutaneous lesions showed severe epithelial hyperplasia and squamous metaplasia, with superficial necrosis, and a myriad of cytoplasmic eosinophilic inclusions in epithelial cells, characteristic of poxvirus infection (Fig. 1C and D). Tracheal swabs (cases #16-055 and #16-069) or cutaneous tissues (cases #16-117 and #16-130) sampled on diseased birds, tested positive for p4b locus shared by all avipoxviruses as well as for fpv140 gene, distinguishing fowlpox virus and canarypox virus (data not shown). Avian Infectious laryngotracheitis (ILT) was excluded on basis of histopathology and PCR.

### 3.2. Whole-genome sequencing

A first test run was performed to validate DNA extraction process, library preparation and sequencing. The sample was obtained from a field isolate propagated on a CAM. A total of 3.87 Gb was produced, 39 625 out of the 502 171 generated sequences were fowlpox-specific and allowed a whole genome alignment having 638X mean depth. Sequencing of non-enriched pox lesions with the MinIon is therefore feasible.

The second and third runs, performed directly on tissues, produced 2.57 Gb and 3.74 Gb, respectively. Read length distribution for the two runs are available as shared data (Figs. S1 and S2, referring to the second and the third run, respectively). All field samples contained avipoxvirus sequences and complete whole genome alignments could be obtained from three out of the seven samples, corresponding to two tracheal and one central nodular cutaneous sample (Table 1; Fig. 2). The three complete genomes were annotated using GATU (Tcherepanov et al., 2006) and deposited in GenBank under accession numbers MF766432, MF766431 and MF766430, for cutaneous lesion #16117-1, respiratory lesion #16069-1 and respiratory lesion #16055-3, respectively. Compared to fowlpox reference genome, no gene was deleted or inserted in any of the three complete genomes, the genomic structure being strictly identical to FWPV.

Due to poor pox DNA abundance in the lung sample or in one of the peripheral nodular cutaneous sample and the simultaneous excess of cellular DNA, we could not obtain a whole genome alignment from these tissues. Sequence data after quality filtering and sequence alignment is summarized in Table 1. Briefly, the sequencing of the cutaneous sample produced 3 905 fowlpox virus sequences out of 163 824; the sequencing of the tracheas generated 3 265 and 2 234 fowlpox virus sequences out of 124 534 and 141 670. The longest mapped read was obtained with the cutaneous sample and sized 61 kb.

Considering the previous results, *de novo* assemblies were performed on the cutaneous lesion 16117-1, the respiratory lesion 16069-1 and on the respiratory lesion 16055-3 samples. The best results were obtained with Minimap2 for the first sample and with SMARTdenovo for the two others. Except for 16055-3 sample whose *de novo* assembly is obtained with only one full contig, *de novo* assemblies consisted in two or more contigs.

The error rates were calculated directly from the raw reads using Blasr aligner (Chaisson and Tesler, 2012). The reads mapping the reference genome had the following error rates: 18.4% for 16069-1 sample, 13% for 16117-1 sample and 13.8% for 16055-3 sample.

### 3.3. Whole-genome phylogenetic analysis

A table of genetic distances (Table 2), as well as the neighbor-joining tree, were derived from whole avipoxvirus genomes (Sarker et al., 2017) and confirmed the close relationship between viruses isolated in this study and fowlpox virus genome reference (GenBank accession number AF198100) (Fig. 3). This result was confirmed using a maximum Likelihood model implemented in MEGA7 (data not shown).

**Table 1**
Sequence data after quality filtering and sequence alignment.

| | Filtered reads | Reads mean length (pb) | Reads mapping fowlpox genome | Genome coverage (%) | Identity % vs ref. genome (NC_002188.1) | Mean depth | Longest mapped read (bp) | Genome size (bp) | Error rate (%) |
|---|---|---|---|---|---|---|---|---|---|
| Amplified isolate on CAM | 502 171 | 3 630 | 39 625 | 100 | 100 | 638X | 77 063 | 288 539 | |
| Cutaneous lesion 16117-1 | 163 824 | 1 352 | 3 905 | 100 | 99,7 | 22X | 61 912 | 288 539 | 7,9% |
| Respiratory lesion 16069-1 | 124 534 | 2 568 | 3 265 | 100 | 99,8 | 30X | 49 439 | 288 539 | 8,7% |
| Respiratory lesion 16055-3 | 141670 | 3 253 | 2 234 | 100 | 99,8 | 19X | 37 780 | 288 539 | 8,5% |
| Cutaneous lesion 16130-2 | 148 398 | 3998 | 1 283 | 63 | – | – | 36 390 | | |
| Peripheral nodular cutaneous tissue 16130-3 | 127 240 | 5187 | 24 | 28 | – | – | 17 049 | | |
| Peripheral nodular cutaneous tissue 16117-2 | 184 368 | 4218 | 85 | 62 | – | – | 39 992 | | |
| Respiratory lesion (lung) 16055-1 | 158 086 | 6004 | 1 182 | 69 | – | – | 28 036 | | |

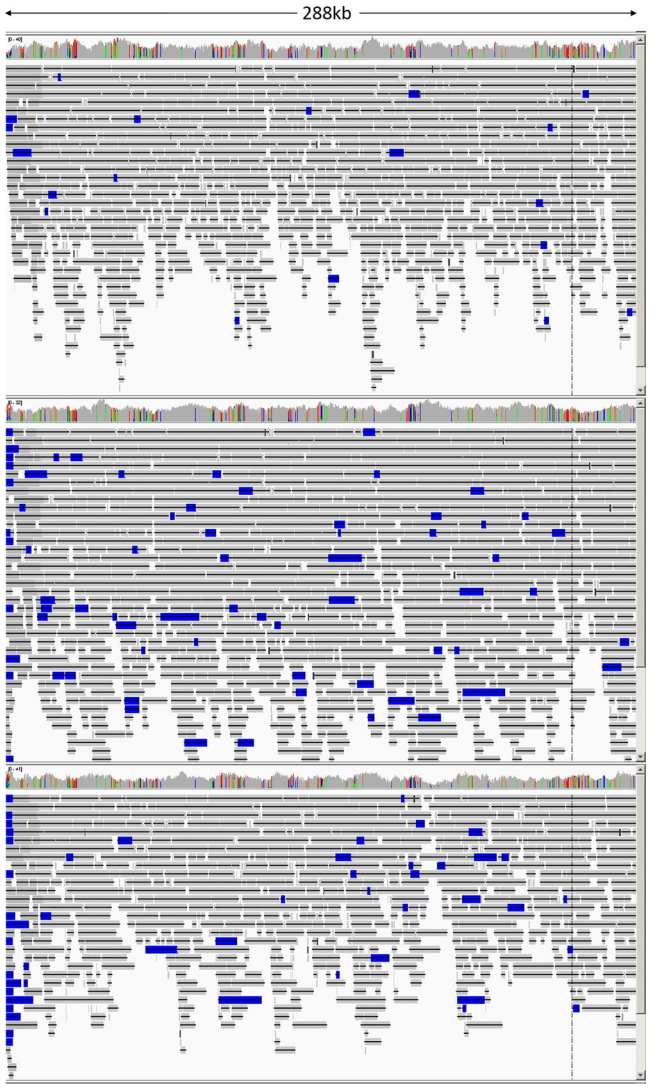


**Fig. 2.** Sequence alignment display on the reference fowlpox genome with IGV for three samples.

## 4. Discussion and conclusion

We readily generated whole APV genomes from three out of seven field samples corresponding to cutaneous or tracheal lesions, without any isolation or PCR-based enrichment. Long reads sequencing may be achieved on the Oxford Nanopore MinION using preferably traditional DNA extraction techniques (Sambrook and Russell, 2001 phenol-chloroform extraction/purification protocol), in order to avoid the damages caused by column-based extraction methods. These genomes are highly similar to the prototype fowlpox reference strain NC_002188.1, including its REV insertion. The significance of REV remains unclear: it could putatively induce an increased virulence (Zhao et al., 2014) or poor fowlpox vaccine efficacy (Koo et al., 2013; Singh et al., 2000) but its seems actually much common in fowlpoxviruses (Tadese et al., 2008). Here again, a genome-based surveillance will be of great help to assess genetic diversity and significance of these retroviral insertions.

Our hypothesis was that active poxviral lesions should show significant viral-to-cellular ratios, which makes possible direct sequencing without need of enrichment. Indeed, fowlpox virus reads loads ranged from 0.75% to 2.62%. The long read size eases the assembly step and lowers the bioinformatics capacity requirements and processing time compared to huge sets of 2nd generation short reads. We had tentatively included peripheral cutaneous lesions or lung tissue in respiratory

**Table 2**
Genetic distances between avipoxvirus whole genomes.

| | AF198100 FWPV | MF766430 RESP. LESION | MF766431 RESP. LESION | MF766432 CUT. LESION | KJ801920 FEP2 | KJ859677 PEPV | MF67879 FGPV6 | KP728110 TKPV | AY318871 CNPV | KX857215 SWPV-2 |
|---|---|---|---|---|---|---|---|---|---|---|
| MF766430 RESP. LESION | 0,1% | | | | | | | | | |
| MF766431 RESP. LESION | 0,1% | 0,0% | | | | | | | | |
| MF766432 CUT. LESION | 0,1% | 0,0% | 0,0% | | | | | | | |
| KJ801920 FEP2 | 14,5% | 14,5% | 14,5% | 14,5% | | | | | | |
| KJ859677 PEPV | 14,9% | 14,8% | 14,8% | 14,8% | 5,5% | | | | | |
| MF67879 FGPV6 | 14,2% | 14,2% | 14,2% | 14,2% | 5,9% | 6,0% | | | | |
| KP728110 TKPV | 46,4% | 46,4% | 46,3% | 46,3% | 45,2% | 45,4% | 45,7% | | | |
| AY318871 CNPV | 47,2% | 47,2% | 47,2% | 47,2% | 47,9% | 47,1% | 48,0% | 50,4% | | |
| KX857215 SWPV-2 | 47,1% | 47,1% | 47,0% | 47,0% | 47,6% | 46,8% | 47,8% | 50,4% | 1,1% | |
| KX857216 SWPV-1 | 46,4% | 46,4% | 46,4% | 46,4% | 47,2% | 45,9% | 47,2% | 49,5% | 31,1% | 31,0% |

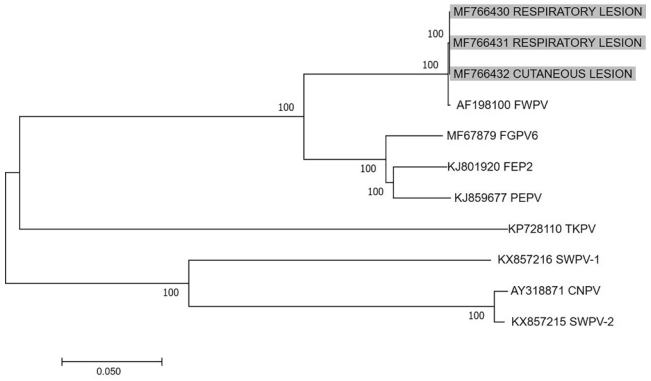


**Fig. 3.** Neighbor-joining phylogenetic tree of avipoxviruses whole genomes sequences. The neighbor-joining phylogenetic tree was constructed with the Kimura 2-parameters model and bootstrap values are shown. The 3 sequences obtained in the present study are highlighted in grey.

forms, but viral loads were much lower in both tissues, which is in accordance with the pathological pictures. The selection of the most relevant samples is a critical step before implementation of any metagenomic protocol: clinical signs, gross and microscopic lesions may be very useful to adapt, for each case, the collection (animals, tissues, time of sampling) and optimize the pathogens/host nucleid acids ratio and hence, the coverage of pathogens genomes.

We investigated the implementation of *de novo* assembly in our pipeline: the two tools, Minimap2 and SMARTdenovo, produced consistent results, allowing an accurate identification of the pathogen thanks to the generation of contigs sizing up to 290 kb. However, despite a similarity very close to the consensus sequences produced with IGV software, the *de novo* assembly did not result in a benefit in terms of timeliness nor accuracy and was not further investigated (data not shown).

ONT MinION is a portable NGS platform, able to generate up to 10 Gigabases per flowcell within a few hours and so specially dedicated to the diagnostic field. The low accuracy due to systematic error is still a well-known drawback of Oxford Nanopore technology. Anyway, yield and accuracy get continuously better, making new applications accessible for veterinary surveillance. Furthermore, regarding applications in the field of diagnostic and epidemiological surveillance of pathogens, a remaining rate of nucleotides mismatches can be accepted since it does not impact typing and decision-making.

Based on our findings, ONT could be readily applied to whole-genome sequencing of other poxviruses, such as Myxoma virus in rabbits, Lumpy skin disease virus in ruminants, and potentially zoonotic poxviruses, such as Monkeypoxvirus. Recently, a combination of Illumina and ONT protocols has been successfully applied to sequencing of a 128 kbp genome of parapoxvirus (Günther et al., 2017). Global surveillance of emerging poviruses and comprehension of their evolution will dramatically benefit from this increasing availability of complete genomes.

## Acknowledgments

This work was performed in the framework of the LabCom VIRAL, associating ENVT, INRA and FILAVIE and funded by the French National Research Agency (ANR-15-LCV1-0003-01). We acknowledge the very efficient, long-term, collaboration with Labovet Veterinary Practice, Réseau Cristal, Les Herbiers, France.

## References

Bányai, K., Palya, V., Dénes, B., Glávits, R., Ivanics, É., Horváth, B., Farkas, S.L., Marton, S., Bálint, Á., Gyuranecz, M., Erdélyi, K., Dán, Á., 2015. Unique genomic organization of a novel Avipoxvirus detected in turkey (Meleagris gallopavo). Infect. Genet. Evol.

J. Mol. Epidemiol. Evol. Genet. Infect. Dis. 35, 221–229. https://doi.org/10.1016/j.meegid.2015.08.001.
Cavener, D.R., 1987. Comparison of the consensus sequence flanking translational start sites in Drosophila and vertebrates. Nucleic Acids Res. 15, 1353–1361.
Chaisson, M.J., Tesler, G., 2012. Mapping single molecule sequencing reads using basic local alignment with successive refinement (BLASR): application and theory. BMC Bioinf. 13https://doi.org/10.1186/1471-2105-13-238. 238.
Günther, T., Haas, L., Alawi, M., Wohlsein, P., Marks, J., Grundhoff, A., Becher, P., Fischer, N., 2017. Recovery of the first full-length genome sequence of a parapoxvirus directly from a clinical sample. Sci. Rep. 7, 3734. https://doi.org/10.1038/s41598-017-03997-y.
Gyuranecz, M., Foster, J.T., Dán, Á., Ip, H.S., Egstad, K.F., Parker, P.G., Higashiguchi, J.M., Skinner, M.A., Höfle, U., Kreizinger, Z., Dorrestein, G.M., Solt, S., Sós, E., Kim, Y.J., Uhart, M., Pereda, A., González-Hein, G., Hidalgo, H., Blanco, J.-M., Erdélyi, K., 2013. Worldwide phylogenetic relationship of avian poxviruses. J. Virol. 87, 4938–4951. https://doi.org/10.1128/JVI.03183-12.
Huw Lee, L., Hwa Lee, K., 1997. Application of the polymerase chain reaction for the diagnosis of fowl poxvirus infection. J. Virol. Methods 63, 113–119.
Katoh, K., Misawa, K., Kuma, K., Miyata, T., 2002. MAFFT: a novel method for rapid multiple sequence alignment based on fast Fourier transform. Nucleic Acids Res. 30, 3059–3066.
Koo, B.S., Lee, H.R., Jeon, E.O., Jang, H.S., Han, M.S., Min, K.C., Lee, S.B., Kim, J.J., Mo, I.P., 2013. An outbreak of lymphomas in a layer chicken flock previously infected with fowlpox virus containing integrated reticuloendotheliosis virus. Avian Dis. 57, 812–817. https://doi.org/10.1637/10551-041113-Case.R1.
Lawson, B., Lachish, S., Colvile, K.M., Durrant, C., Peck, K.M., Toms, M.P., Sheldon, B.C., Cunningham, A.A., 2012. Emergence of a novel avian pox disease in British tit species. PloS One 7https://doi.org/10.1371/journal.pone.0040176. e40176.
Le Loc'h, G., Ducatez, M.F., Camus-Bouclainville, C., Guérin, J.-L., Bertagnoli, S., 2014. Diversity of avipoxviruses in captive-bred Houbara bustard. Vet. Res. 45https://doi.org/10.1186/s13567-014-0098-3. 98.
Lecis, R., Secci, F., Antuofermo, E., Nuvoli, S., Scagliarini, A., Pittau, M., Alberti, A., 2017. Multiple gene typing and phylogeny of avipoxvirus associated with cutaneous lesions in a stone curlew. Vet. Res. Commun. 41, 77–83. https://doi.org/10.1007/s11259-016-9674-5.
Lefkowitz, E.J., Wang, C., Upton, C., 2006. Poxviruses: past, present and future. Virus Res. 117, 105–118. https://doi.org/10.1016/j.virusres.2006.01.016.
Li, H., 2017. Minimap2: Pairwise Alignment for Nucleotide Sequences. ArXiv170801492 Q-Bio. .
Li, H., Durbin, R., 2009. Fast and accurate short read alignment with Burrows-Wheeler transform. Bioinf. Oxf. Engl. 25, 1754–1760. https://doi.org/10.1093/bioinformatics/btp324.
Li, H., Handsaker, B., Wysoker, A., Fennell, T., Ruan, J., Homer, N., Marth, G., Abecasis, G., Durbin, R., 1000 Genome Project Data Processing Subgroup, 2009. The sequence alignment/map format and SAMtools. Bioinf. Oxf. Engl. 25, 2078–2079. https://doi.org/10.1093/bioinformatics/btp352.
Loman, N.J., Quinlan, A.R., 2014. Poretools: a toolkit for analyzing nanopore sequence data. Bioinf. Oxf. Engl. 30, 3399–3401. https://doi.org/10.1093/bioinformatics/btu555.
Robinson, J.T., Thorvaldsdóttir, H., Winckler, W., Guttman, M., Lander, E.S., Getz, G., Mesirov, J.P., 2011. Integrative genomics viewer. Nat. Biotechnol. 29, 24–26. https://doi.org/10.1038/nbt.1754.
Ruan, J., 2018. Smartdenovo: Ultra-fast De Novo Assembler Using Long Noisy Reads.
Sambrook, P., Russell, D., 2001. 3rd ed. Molecular Cloning: A Laboratory Manual, vols. 1–3 M8265 [WWW Document]. URL (Accessed 10.11.17).
Sarker, S., Das, S., Lavers, J.L., Hutton, I., Helbig, K., Imbery, J., Upton, C., Raidal, S.R., 2017. Genomic characterization of two novel pathogenic avipoxviruses isolated from pacific shearwaters (Ardenna spp.). BMC Genomics 18, 298. https://doi.org/10.1186/s12864-017-3680-z.
Singh, P., Kim, T.J., Tripathy, D.N., 2000. Re-emerging fowlpox: evaluation of isolates from vaccinated flocks. Avian Pathol. J. WVPA 29, 449–455. https://doi.org/10.1080/030794500750047207.
Tadese, T., Fitzgerald, S., Reed, W.M., 2008. Detection and differentiation of re-emerging fowlpox virus (FWPV) strains carrying integrated reticuloendotheliosis virus (FWPV-REV) by real-time PCR. Vet. Microbiol. 127, 39–49. https://doi.org/10.1016/j.vetmic.2007.08.012.
Tcherepanov, V., Ehlers, A., Upton, C., 2006. Genome Annotation Transfer Utility (GATU): rapid annotation of viral genomes using a closely related reference genome. BMC Genomics 7, 150. https://doi.org/10.1186/1471-2164-7-150.
Vaser, R., Sović, I., Nagarajan, N., Šikić, M., 2017. Fast and accurate de novo genome assembly from long uncorrected reads. Genome Res. 27, 737–746. https://doi.org/10.1101/gr.214270.116.
Zhao, K., He, W., Xie, S., Song, D., Lu, H., Pan, W., Zhou, P., Liu, W., Lu, R., Zhou, J., Gao, F., 2014. Highly pathogenic fowlpox virus in cutaneously infected chickens, China. Emerg. Infect. Dis. 20, 1208–1210. https://doi.org/10.3201/eid2007.131118.